

Rapid emergence of subaerial landmasses and onset of a modern hydrologic cycle 2.5 billion years ago

I. N. Bindeman^{1*}, D. O. Zakharov¹, J. Palandri¹, N. D. Greber², N. Dauphas³, G. J. Retallack¹, A. Hofmann⁴, J. S. Lackey⁵ & A. Bekker^{4,6}

The history of the growth of continental crust is uncertain, and several different models that involve a gradual, decelerating, or stepwise process have been proposed^{1–4}. Even more uncertain is the timing and the secular trend of the emergence of most landmasses above the sea (subaerial landmasses), with estimates ranging from about one billion to three billion years ago^{5–7}. The area of emerged crust influences global climate feedbacks and the supply of nutrients to the oceans⁸, and therefore connects Earth's crustal evolution to surface environmental conditions^{9–11}. Here we use the triple-oxygen-isotope composition of shales from all continents, spanning 3.7 billion years, to provide constraints on the emergence of continents over time. Our measurements show a stepwise total decrease of 0.08 per mille in the average triple-oxygen-isotope value of shales across the Archaean–Proterozoic boundary. We suggest that our data are best explained by a shift in the nature of water–rock interactions, from near-coastal in the Archaean era to predominantly continental in the Proterozoic, accompanied by a decrease in average surface temperatures. We propose that this shift may have coincided with the onset of a modern hydrological cycle owing to the rapid emergence of continental crust with near-modern average elevation and aerial extent roughly 2.5 billion years ago.

Changes in Earth's surface environments between about 2.5 billion years ago (2.5 Gyr ago) and 2.32 Gyr ago are recorded in numerous isotopic and elemental systems, which point to a dramatic change in the oxygenation of the atmosphere and oceans at that time^{9,10}. These changes were associated with a series of three to four 'Snowball Earth' glaciations^{11,12}, whose origin and driving forces are still debated. The major geochemical and biogeochemical rearrangements in Earth's surface environments at the Archaean–Proterozoic boundary (2.5 Gyr ago) also left numerous signatures in the geological record. Among these signatures is a steep rise in the oxygen isotopic $^{18}\text{O}/^{16}\text{O}$ ratio (expressed as $\delta^{18}\text{O}$, the deviation in the ratio in per mille relative to the standard ratio in modern seawater, VSMOW) of shales and zircons in the Late Archaean, followed by a progressively decelerating increase in these values into the Phanerozoic^{13,14}. This first-order trend was modulated by the assembly and break-up of supercontinents¹⁴. However, it is unclear how these changes in $\delta^{18}\text{O}$ (as well as other parameters) relate to the isotopic evolution of continental crust, to the evolution of meteoric water, or to weathering conditions at Earth's surface.

We present here triple-oxygen-isotope measurements of shales, which are the dominant sedimentary rocks on Earth and the products of the chemical and physical weathering of landmasses that are exposed to the atmosphere. Shales consist mainly of clay minerals, secondary quartz and unmodified detrital minerals; studies of shales have been used previously to constrain the chemical evolution of Earth's crust through time^{1,3,8,15,16}. The triple-oxygen-isotope composition of shales is expressed here as $\delta^{18}\text{O}$ and $\Delta^{17}\text{O}$ values; the latter parameter reflects linearized deviations in per mille (‰) of $^{17}\text{O}/^{16}\text{O}$ ratios relative to a mass-dependent $^{17}\text{O}/^{16}\text{O}$ versus $^{18}\text{O}/^{16}\text{O}$ fractionation

line with a reference slope of 0.5305 (see Fig. 1 and Supplementary Information section 'Methods' for details). Both parameters are independent functions of temperature and oxygen-isotope variations and fractionation processes in surface environments^{17–19}.

The $\delta^{18}\text{O}$ – $\Delta^{17}\text{O}$ signature of bulk shales is defined by: first, the proportions of detrital versus authigenic mineral components; second, the temperature of weathering and diagenesis, which affects isotopic fractionation factors; and third, the isotopic composition of the altering water (Fig. 1). Although used extensively in the past, $^{18}\text{O}/^{16}\text{O}$ ratios alone^{14,20,21} are insufficient for disentangling the impact of these various processes on the shale composition. However, as we show here, the combined use of $\delta^{18}\text{O}$ and $\Delta^{17}\text{O}$ removes the ambiguities associated with using $\delta^{18}\text{O}$ alone, and allows us to reconstruct past surface conditions and the composition of meteoric waters involved in weathering.

The shale samples used here are the same as those used previously¹⁴, with the addition of 30 composite samples (formation-averaged) and 10 individual recent and Archaean samples (Fig. 1, Extended Data Tables 1–3). These 278 samples were collected from outcrops and drill holes on all continents and span 3.7 Gyr. The measured $\delta^{18}\text{O}$ values agree with previously determined values for shales and other sediment types and detrital zircons (Fig. 2)^{7,13,14,16}. The bulk shales cover a large field in the $\delta^{18}\text{O}$ – $\Delta^{17}\text{O}$ space (Fig. 1). The observed $\Delta^{17}\text{O}$ values range from those typical of mantle and crust (–0.05‰ to –0.09‰)^{18,22} to –0.3‰. Furthermore, the triple-oxygen-isotope data of shales fall on different mass-dependent fractionation lines, with slopes between the $^{18}\text{O}/^{16}\text{O}$ and $^{17}\text{O}/^{16}\text{O}$ ratios ranging from 0.529 to 0.516 (Fig. 1, Supplementary Information)—values that encompass the entire range of slopes described previously for mass-dependent processes on Earth²².

Our results confirm a gradual trend of increasing $\delta^{18}\text{O}$ values from 3.7 Gyr ago towards modern times. Meanwhile, the $\Delta^{17}\text{O}$ values of shales exhibit a stepwise shift to more negative and more diverse values during and after the Archaean–Proterozoic transition (Fig. 2a). Shales older than 2.5 Gyr define an average $\Delta^{17}\text{O}$ value of $-0.047\text{‰} \pm 0.012\text{‰}$ ($\pm 2\sigma$), while shales younger than 2.2 Gyr—deposited in later stages and after the Great Oxidation Event (GOE) roughly 2.32 Gyr ago, during which O_2 appeared in the atmosphere—yield an average $\Delta^{17}\text{O}$ value of $-0.118\text{‰} \pm 0.024\text{‰}$. This difference in the triple-oxygen-isotope composition of the two age groups cannot be explained solely by different equilibration temperatures, or by the mixing of different proportions of variably weathered detrital materials, as the shale record cuts across the $\delta^{18}\text{O}$ – $\Delta^{17}\text{O}$ trends defined by these processes (Fig. 1), requiring different initial $\delta^{18}\text{O}$ meteoric waters. Moreover, there is no difference in the chemical index of alteration (CIA²³) or in the proportions of minerals (determined by X-ray diffraction, XRD) of the studied shales across the GOE (Extended Data Table 2, Fig. 2) that could explain the observed shift in the $\Delta^{17}\text{O}$ values of the shales. The invariable titanium-isotope values⁸ and constant characteristic elemental ratios of the studied shales¹⁴ (Extended Data Fig. 1) suggest that

¹Department of Earth Sciences, University of Oregon, Eugene, OR, USA. ²Department of Earth Sciences, University of Geneva, Geneva, Switzerland. ³Origins Laboratory, Department of the Geophysical Sciences and Enrico Fermi Institute, The University of Chicago, Chicago, IL, USA. ⁴Department of Geology, University of Johannesburg, Auckland Park, South Africa. ⁵Department of Geology, Pomona College, Claremont, CA, USA. ⁶Department of Earth Sciences, University of California, Riverside, CA, USA. *e-mail: bindeman@uoregon.edu

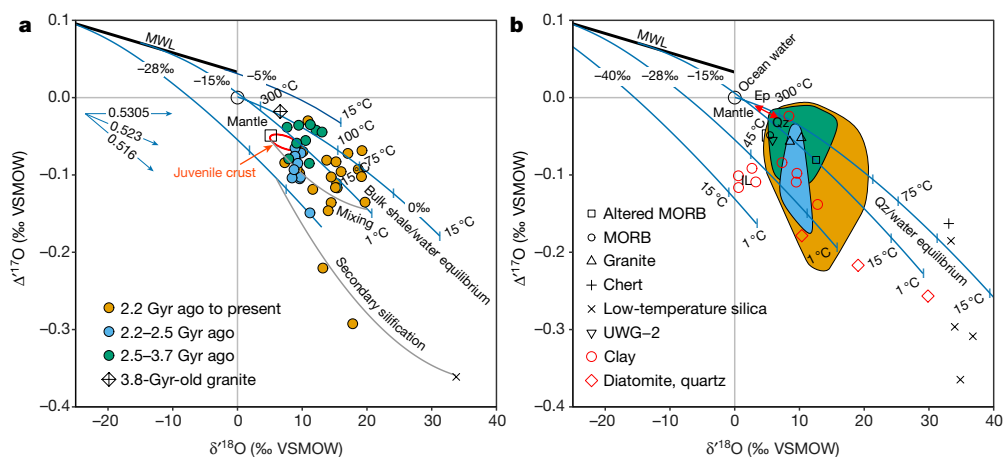


Fig. 1 | Triple-oxygen-isotope systematics of ancient and modern terrestrial materials. a, Ancient materials. b, Modern materials.

The coloured fields in **b** correspond to the ancient-shale data shown with coloured dots in **a**. The concave blue curves represent isotopic fractionation between weathering products and meteoric water. The labels on the blue curves show the $\delta^{18}\text{O}$ values of meteoric waters, ranging from -5‰ to -40‰ , and of modern ocean water (black open circle; 0‰). The modern meteoric water line is labelled MWL. In **a**, the fractionation curves for bulk shale/water equilibration were constructed assuming a weathering product of 70% illite and 30% quartz (see Supplementary Information). In **b**, the fractionation curves are based on experimentally determined quartz/water triple-oxygen-isotope fractionations¹⁹. In **a**, the grey convex mixing curve connects unweathered terrestrial materials (such as mantle or upper crust) with the weathering products located

on the blue fractionation lines; the grey secondary silicification curve connects modern high- $\delta^{18}\text{O}$ and low- $\Delta^{17}\text{O}$ materials (such as cherts and sponge spicules; individual data are shown in **b**). In **b**, the various Earth materials analysed here (red symbols) and in refs^{18,19} (black symbols) are normalized to a mantle $\Delta^{17}\text{O}$ value of -0.05‰ ; the double-headed red arrow, with a slope of 0.528, connects coexisting hydrothermal quartz (Qz) and epidote (Ep) from the modern deep-ocean core 504B, which formed at about 300°C in equilibrium with roughly 0‰ seawater. In **a**, the blue arrows and associated values depict the slopes of triple-oxygen fractionation in linearized $\delta^{17}\text{O}$ – $\delta^{18}\text{O}$ space, with the values reflecting logarithmic linearization of the delta scales³² (see Supplementary Information); 0.5305 is characteristic of infinitely high temperatures and smaller slopes are characteristic of lower-temperature fractionations. IL, illite; VSMOW, Vienna Standard Mean Ocean Water.

the parental, atmospherically exposed continental crust undergoing weathering was similar in chemical composition to the modern crust, and has had similar proportions of mafic and felsic rocks since at least 3.5 Gyr ago, with a greater contribution of komatiites in the Archaean^{8,16}. Higher-temperature Archaean oceans²⁴, or a greater contribution of hydrothermal clays to Archaean shales, would result in less-positive $\delta^{18}\text{O}$ and less-negative $\Delta^{17}\text{O}$ values. Although this could help to explain the lower $\delta^{18}\text{O}$ values that we observe²⁴, it cannot explain the vertically extending trend of lower $\Delta^{17}\text{O}$ values (Fig. 1, Extended Data Fig. 2) or the step change in $\Delta^{17}\text{O}$ values 2.5 Gyr ago (Fig. 2). In addition, our shales show no geological or mineralogical evidence for a substantial change in hydrothermal contribution or weathering intensity in the CIA parameter across the Archaean–Proterozoic boundary¹⁴. Taking a cue from the modern world, where meteoric water shows variable $\delta^{18}\text{O}$ – $\Delta^{17}\text{O}$ compositions¹⁷, the simplest explanation for some of the oxygen-isotope variations measured in ancient shales is that they were in part inherited from the waters involved in rock alteration on the continents.

We applied recently established isotope-fractionation factors for $^{18}\text{O}/^{16}\text{O}$ and $^{17}\text{O}/^{16}\text{O}$ between quartz and water at different temperatures¹⁹ to transform our measured, raw $\delta^{18}\text{O}$ – $\Delta^{17}\text{O}$ data for shales into actual surface weathering conditions. We also calculated the equilibrium fractionation of oxygen isotopes between bulk shale and water, at different temperatures and initial $\delta^{18}\text{O}$ – $\Delta^{17}\text{O}$ water values along the meteoric water line (MWL; Fig. 1, Extended Data Figs. 3–5). Oxygen-isotope fractionation between clay minerals and water under low temperatures is less than that for water and secondary quartz²⁰, but the two mineral/water pairs follow the same fractionation law (ref. 18; see also Supplementary Information and Extended Data Fig. 6). The bulk shale/water fractionation lines (blue curves in Fig. 1a) define a negative slope in $\delta^{18}\text{O}$ – $\Delta^{17}\text{O}$ space. Mixing detrital material derived from the continental crust with authigenic minerals follows a subparallel curve (grey line in Fig. 1a) within the field defined by the isotope-fractionation curves. The calculation shows that variations in temperature, in the initial oxygen-isotope composition of altering waters, and in mixing ratios between detrital material and weathering

products can explain the overall trend and negative co-variations in our data.

The proportion of weathering products in a shale can be assessed independently via its mineralogical composition (through XRD) and/or its chemical composition (such as through the CIA²³). Combining this estimate with the $\delta^{18}\text{O}$ and $\Delta^{17}\text{O}$ values of the shales and the pristine detrital components (igneous rocks) allows us to calculate, by mass balance, the $\delta^{18}\text{O}$ and $\Delta^{17}\text{O}$ values of the weathering products (Extended Data Fig. 3). The CIA index has remained nearly constant through time¹⁴ (Extended Data Fig. 7), suggesting that a secular trend in weathering intensity is unlikely to introduce a systematic bias in this approach. The equations for isotopic fractionation during water–rock interactions and the equation of the MWL in $\delta^{18}\text{O}$ – $\Delta^{17}\text{O}$ space (Fig. 1) can be used to independently calculate the water–rock interaction temperature and the oxygen-isotopic composition ($\delta^{18}\text{O}_\text{w}$ and $\Delta^{17}\text{O}_\text{w}$) of waters involved in weathering and diagenesis (Extended Data Figs. 3, 4). This approach is likely to be oversimplified, because detrital components in shale precursors were probably altered by a range of meteoric and diagenetic waters at different temperatures in watersheds. But, given that we compare shales with shales, all of which have comparable CIAs, these complexities do not affect the first-order interpretations afforded by quantitative modelling.

We find that the temperatures of interacting water and rock derived from the inversion of shale $\delta^{18}\text{O}$ – $\Delta^{17}\text{O}$ values were higher during the Archaean than after it (Extended Data Fig. 5). This modelling exercise also shows that—although our measurements reveal trends towards heavier average $\delta^{18}\text{O}$ and lighter average $\Delta^{17}\text{O}$ values in shales over time—the waters involved in surface alteration and weathering processes became lighter in $\delta^{18}\text{O}$, heavier in $\Delta^{17}\text{O}$, and more variable in both $\delta^{18}\text{O}$ and $\Delta^{17}\text{O}$ after roughly 2.5 Gyr ago. Although the quantitative analysis makes important simplifications, it does capture the essential features of weathering conditions on continents through time.

Another explanation for the stepwise change in $\Delta^{17}\text{O}$ values during the GOE could be the appearance of atmospheric oxygen and ozone.

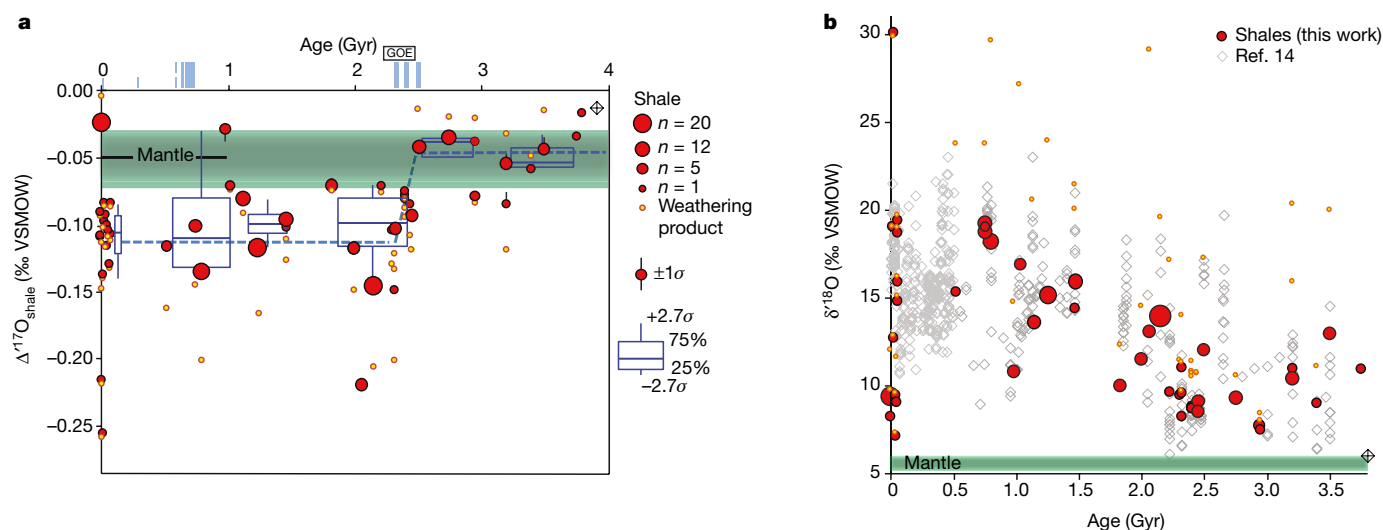


Fig. 2 | Oxygen-isotopic compositions of shales through time. **a**, $\Delta^{17}\text{O}$ record of shales (red points) and calculated oxygen-isotopic composition of weathering products (yellow points), showing a stepwise change in composition between 2.5 Gyr ago and 2.2 Gyr ago. The blue dashed lines represent the mean $\Delta^{17}\text{O}$ values, weighted by the composite sample size (n), for shales before 2.5 Gyr ago and after 2.2 Gyr ago. The boxes represent the medians, interquartile ranges and extreme values (see legend). A t -test reveals that the Archaean and post-Archaean $\Delta^{17}\text{O}$

values are statistically distinct ($0.004 < P < 0.02$, well below a statistical significance value of 0.05). We attribute the different $\delta^{18}\text{O}$ and $\Delta^{17}\text{O}$ values of pre- and post-Archaean shales in this diagram to a change from a coast-dominated to a more continental hydrological cycle and weathering conditions (see text for details). The blue vertical bars at the top indicate major glacial episodes. **b**, $\delta^{18}\text{O}$ record of shales (red points) from our dataset superimposed on the dataset from ref. ¹⁴ (white diamonds).

The formation of ozone with highly positive $\Delta^{17}\text{O}$ values ($+30\text{‰}$ to $+100\text{‰}$) via ultraviolet photolysis in the stratosphere leaves atmospheric oxygen with the slightly negative $\Delta^{17}\text{O}$ value of -0.3‰ in today's 21 vol% oxygen atmosphere^{22,25}, but probably much less in Proterozoic conditions of less than 1 vol% oxygen. However, not only was the atmospheric $\Delta^{17}\text{O}$ signal small, there is also no mechanism by which to transfer this signature into the meteoric water cycle and hence into crustal silicate weathering products such as shales.

As argued above, we favour an explanation by which the difference in the $\Delta^{17}\text{O}$ values of pre- and post-GOE shales occurred through a change in the meteoric water cycle (Fig. 3). Starting roughly at the Archaean–Proterozoic transition, the emerged crust would have interacted with waters that had more variable and on average more negative $\delta^{18}\text{O}_\text{W}$ values and more positive $\Delta^{17}\text{O}_\text{W}$ values than before the GOE (with $\Delta^{17}\text{O}_\text{W}$ shifted by approximately $+0.1\text{‰}$). The observed shift in the triple-oxygen-isotope composition of shales would also have required lower post-GOE surface temperatures (Extended Data Fig. 5). This is broadly consistent with the findings of previous studies of $\delta^{18}\text{O}$ values in cherts²⁴.

In the modern world, the oxygen-isotope composition of precipitation depends on the cumulative history of water loss from the air parcel

that is travelling inland away from the coasts towards higher latitudes and higher altitudes (<http://www.waterisotopes.org>), resulting in lower $\delta^{18}\text{O}_\text{W}$ values, higher $\Delta^{17}\text{O}_\text{W}$ values, and more diverse compositions overall¹⁷ (as in the MWL on Fig. 1). This combined effect, which we call ‘continentality’ (Fig. 3), is shown through the shale record's step change that coincides with the Archaean–Proterozoic boundary (Figs. 2a, 3). It is most likely that the observed change in the shale triple-oxygen-isotope record reflects the appearance of larger continents (Fig. 3) and higher elevations from the Proterozoic onwards—a period that is broadly contemporaneous with the final stages in the assembly of the first documented supercontinent, Kenorland^{2,26}, or with the formation of several supercratons^{12,15} immediately before the GOE²⁷. Supercontinent assembly and orogenic events result in high mountain ranges and plateaus, as occurred when India collided with Asia, forming the Himalayas and Tibet. Rising mountains in even quite low to mid latitudes result in precipitation with very light $\delta^{18}\text{O}$ values (<http://www.waterisotopes.org>) that correlate with elevation, with a roughly 2‰–3‰ drop in $\delta^{18}\text{O}$ per kilometre of altitude gain²⁸.

Supporting our interpretations of triple-oxygen variations in shales is the strontium-isotope record of marine carbonates, which suggests

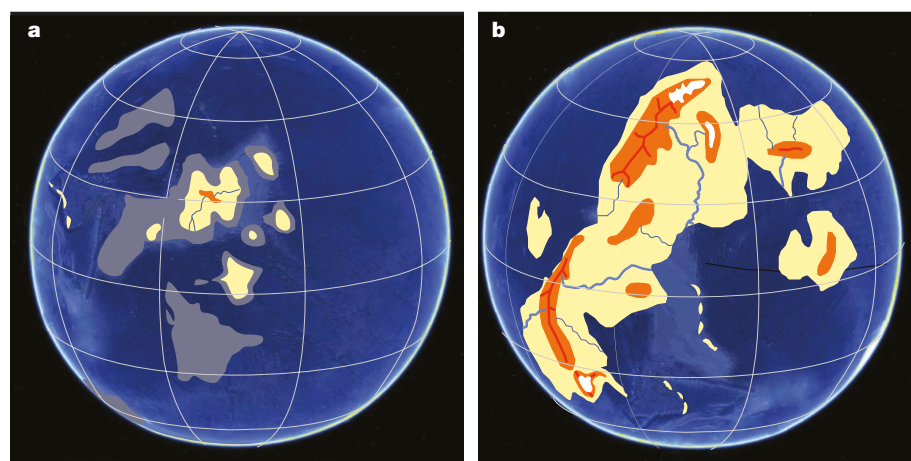


Fig. 3 | Conceptual palaeohypsometry of Archaean and Proterozoic worlds. These images are based on palaeomagnetic and tectonic reconstructions (see refs ^{12,26} and references therein). **a**, The late Archaean era (shortly before 2.5 Gyr ago) during the assembly of the supercontinent Kenorland. **b**, The early/mid Paleoproterozoic era, after the occurrence of the GOE. The oceans are shallower in **a** compared with **b**, and the (excessively flooded) continents are smaller and lower, resulting in different hydrologic and weathering cycles, as described here.

that the area of emerged continental crust increased substantially and irreversibly at roughly the Archaean–Proterozoic boundary²⁹. From a geodynamic perspective, models of a cooling Earth call for a thickening of the lithosphere and the establishment of a higher continental freeboard by about 2.5 Gyr ago owing to increased mantle viscosity^{5,30,31}. The emergence of large landmasses (Fig. 3) would also have led to a larger weathering sink for carbon dioxide, which occurred at greater concentrations in the Archaean, resulting in a transition to moderate surface temperatures after the GOE. We conclude that this set of large-scale tectonic and near-surface changes best explains the observed shift in the $\delta^{18}\text{O}$ – $\Delta^{17}\text{O}$ composition of shales between 2.5 Gyr ago and 2.2 Gyr ago (Fig. 2).

The rapid increase in Earth's subaerial surface and overall hypsometry 2.5 Gyr ago that we infer here (Fig. 3) would have also increased Earth's albedo, the flux of nutrients to the oceans⁸ from continents undergoing subaerial weathering, and the extent of continental margins, additionally resulting in a higher rate of burial of organic carbon and reducing the concentration of carbon dioxide in the air. Together, these changes could have contributed to the cooling of the planet and to the snowball glaciations of the early Palaeoproterozoic, followed by the GOE, highlighting how Earth's interior could have influenced surface redox conditions and chemistry. The most dramatic change in Earth's history was marked by a transition from hot and largely anoxic surface conditions to an oxygenated atmosphere with moderate surface temperatures. Our study suggests that this transition might have been modulated by long-term cooling of the subcontinental mantle and lithosphere, rendering it capable of supporting a thicker crust^{1,2,30,31}. This would have led to the emergence of extensive landmasses at the Archaean–Proterozoic boundary, with life and surface conditions adjusting to—rather than triggering—the change in atmospheric oxygen concentrations.

Data availability

Data are provided in Extended Data Tables 1–3.

Online content

Any Methods, including any statements of data availability and Nature Research reporting summaries, along with any additional references and Source Data files, are available in the online version of the paper at <https://doi.org/10.1038/s41586-018-0131-1>.

Received: 2 October 2017; Accepted: 7 March 2018;

Published online 23 May 2018.

1. Taylor, S. R. & McLennan, S. M. The geochemical evolution of the continental crust. *Rev. Geophys.* **33**, 241–265 (1995).
2. Condie, K. C. *Plate Tectonics and Crustal Evolution* 3rd edn (Pergamon Press, Oxford, 2013).
3. Belousova, E. A. et al. The growth of the continental crust: constraints from zircon Hf-isotope data. *Lithos* **119**, 457–466 (2010).
4. Keller, C. B., Schoene, B., Barboni, M., Samperton, K. M. & Husson, J. M. Volcanic–plutonic parity and the differentiation of the continental crust. *Nature* **523**, 301–307 (2015).
5. Dhuime, B., Wuestefeld, B. & Hawkesworth, C. J. Emergence of modern continental crust about 3 billion years ago. *Nat. Geosci.* **8**, 552–555 (2015).
6. Lee, C.-T. A. et al. Deep mantle roots and continental emergence: implications for whole-Earth elemental cycling, long-term climate, and the Cambrian explosion. *Int. Geol. Rev.* **60**, 431–448 (2017).
7. Hawkesworth, C. J., Cawood, P. A., Dhuime, B. & Kemp, A. I. S. Earth's continental lithosphere through time. *Annu. Rev. Earth Planet. Sci.* **45**, 169–198 (2017).
8. Greber, N. D. et al. Titanium isotopic evidence for felsic crust and plate tectonics 3.5 billion years ago. *Science* **357**, 1271–1274 (2017).
9. Farquhar, J. & Wing, B. A. The terrestrial record of stable sulphur isotopes: a review of the implications for evolution of Earth's sulphur cycle. *Geol. Soc. Lond. Spec. Publ.* **248**, 167–177 (2005).
10. Bekker, A. et al. Dating the rise of atmospheric oxygen. *Nature* **427**, 117–120 (2004).
11. Hoffman, P. F. The Great Oxidation and a Siderian snowball Earth: MIFS based correlation of Paleoproterozoic glacial epochs. *Chem. Geol.* **362**, 143–156 (2013).
12. Gumsley, A. P. et al. Timing and tempo of the Great Oxidation Event. *Proc. Natl Acad. Sci. USA* **114**, 1811–1816 (2017).
13. Valley, J. W. et al. 4.4 billion years of crustal maturation: oxygen isotope ratios of magmatic zircon. *Contrib. Mineral. Petrol.* **150**, 561–580 (2005).

14. Bindeman, I. N., Bekker, A. & Zakharov, D. O. Oxygen isotope perspective on crustal evolution on early Earth: a record of Precambrian shales with emphasis on Paleoproterozoic glaciations and Great Oxygenation Event. *Earth Planet. Sci. Lett.* **437**, 101–113 (2016).
15. Bleeker, W. The late Archean record: a puzzle in ca. 35 pieces. *Lithos* **71**, 99–134 (2003).
16. Gaschnig, R. M. et al. Compositional evolution of the upper continental crust through time, as constrained by ancient glacial diamictites. *Geochim. Cosmochim. Acta* **186**, 316–343 (2016).
17. Luz, B. & Barkan, E. Variations of $^{17}\text{O}/^{16}\text{O}$ and $^{18}\text{O}/^{16}\text{O}$ in meteoric waters. *Geochim. Cosmochim. Acta* **74**, 6276–6286 (2010).
18. Pack, A. & Herwartz, D. The triple oxygen isotope composition of the Earth mantle and understanding $\delta^{17}\text{O}$ variations in terrestrial rocks and minerals. *Earth Planet. Sci. Lett.* **390**, 138–145 (2014).
19. Sharp, Z. D. et al. A calibration of the triple oxygen isotope fractionation in the SiO_2 – H_2O system and applications to natural samples. *Geochim. Cosmochim. Acta* **186**, 105–119 (2016).
20. Savin, S. & Epstein, S. The oxygen and hydrogen isotope geochemistry of ocean sediments and shales. *Geochim. Cosmochim. Acta* **34**, 43–63 (1970).
21. Land, L. S. & Lynch, F. L. $\delta^{18}\text{O}$ values of mudrocks: more evidence for an ^{18}O -buffered ocean. *Geochim. Cosmochim. Acta* **60**, 3347–3352 (1996).
22. Bao, H. M., Cao, X. B. & Hayles, J. Triple-oxygen isotopes: fundamental relationships and applications. *Annu. Rev. Earth Planet. Sci.* **44**, 463–492 (2016).
23. Nesbitt, H. W. & Young, G. N. Early Proterozoic climates and plate motions inferred from major element chemistry of lutites. *Nature* **299**, 715–717 (1982).
24. Knauth, L. P. & Lowe, D. R. High Archean climatic temperature inferred from oxygen isotope geochemistry of cherts in the 3.5 Ga Swaziland Supergroup, South Africa. *Geol. Soc. Bull.* **115**, 566–580 (2003).
25. Young, E., Yeung, L. Y. & Kohl, I. On the ^{17}O budget of atmosphere. *Geochim. Cosmochim. Acta* **135**, 102–125 (2014).
26. Mertanen, S. & Pesonen, L. J. in *From the Earth's Core to Outer Space* (ed. Haapala, I.) 11–35 (Springer, Berlin, 2012).
27. Barley, M. E., Bekker, A. & Krapez, B. Late Archean to early Paleoproterozoic global tectonics, environmental change and the rise of atmospheric oxygen. *Earth Planet. Sci. Lett.* **238**, 156–171 (2005).
28. Rowley, D. B., Pierrehumbert, R. & Currie, B. A new approach to stable isotope-based paleoaltimetry: implications for paleoaltimetry and paleohypsometry of the High Himalaya since the Late Miocene. *Earth Planet. Sci. Lett.* **188**, 253–268 (2001).
29. Flament, N., Coltice, N. & Rey, P. F. A case for late-Archaean continental emergence from thermal evolution models and hypsometry. *Earth Planet. Sci. Lett.* **275**, 326–336 (2008).
30. Vlaar, N. J. Continental emergence and growth on a cooling earth. *Tectonophysics* **322**, 191–202 (2000).
31. Korenaga, J., Planavsky, N. J. & Evans, D. A. D. Global water cycle and the coevolution of the Earth's interior and surface environment. *Phil. Trans. R. Soc. A* **375**, 20150393 (2017).
32. Miller, M. F. Isotopic fractionation and the quantification of ^{17}O anomalies in the oxygen three-isotope system: an appraisal and geochemical significance. *Geochim. Cosmochim. Acta* **66**, 1881–1889 (2002).

Acknowledgements This work was supported by National Science Foundation (NSF) grant EAR1447337 and by the University of Oregon. N.D. was supported by NSF grant EAR1502591. A.B. was supported by National Sciences and Engineering Research Council (NSERC) Discovery and Accelerator grants. We thank P. Hoffman, S. Mertanen and D. Evans for discussions about Precambrian palaeogeography and environmental changes; K. Johnson for technical help with vacuum lines; and O. Melnik for help with programming.

Reviewer information Nature thanks C. Hawkesworth and the other anonymous reviewer(s) for their contribution to the peer review of this work.

Author contributions I.N.B. conceived the study and wrote the paper; D.O.Z., J.P. and I.N.B. built the purification line and collected the data; N.D.G. and N.D. provided composite shale samples studied previously for titanium isotopes; A.B., A.H. and G.J.R. provided samples; J.S.L. performed major- and trace-element analyses; I.N.B. and N.D. discussed the inversion approach and I.N.B. implemented the model; D.O.Z. contributed to statistical treatment; A.B., N.D., N.D.G. and G.J.R. contributed to discussions on Precambrian environments and crustal evolution. All authors contributed to writing and editing the paper.

Competing interests The authors declare no competing interests.

Additional information

Extended data is available for this paper at <https://doi.org/10.1038/s41586-018-0131-1>.

Supplementary information is available for this paper at <https://doi.org/10.1038/s41586-018-0131-1>.

Reprints and permissions information is available at <http://www.nature.com/reprints>.

Correspondence and requests for materials should be addressed to I.N.B. **Publisher's note**: Springer Nature remains neutral with regard to jurisdictional claims in published maps and institutional affiliations.